



The scarcity of theoretical and experimental data for TM phosphido complexes makes it difficult to characterize the new class of compounds. Accurate quantum chemical calculations of model compounds and subsequent analyses of the theoretical data can help to provide the missing information. It is now possible to calculate heavy-atom molecules like TM compounds reliably using either classical quantum chemical methods in conjunction with pseudopotentials<sup>10</sup> or density functional theory (DFT).<sup>11</sup> Therefore, we decided to carry out a theoretical study of TM phosphido complexes using both methods.

In this work we report quantum mechanical *ab initio* and DFT calculations of the model compounds [M(P)(NH<sub>2</sub>)<sub>3</sub>] (**1**, **2**), [M(PS)(NH<sub>2</sub>)<sub>3</sub>] (**3**, **4**), [M(P)(NH<sub>2</sub>)<sub>3</sub>(NH<sub>3</sub>)] (**5**, **6**), [M(P)(N<sub>3</sub>N)] (**7**, **8**; N<sub>3</sub>N = [(HNCH<sub>2</sub>CH<sub>2</sub>)<sub>3</sub>N]<sup>3-</sup>), and [M(PS)(NH<sub>2</sub>)<sub>3</sub>(NH<sub>3</sub>)] (**9**, **10**) with M = Mo, W. The goal of this study is to gain insight into the nature of the metal–phosphorus bond. To this end we optimized the geometries of **1**–**10** and calculated the <sup>31</sup>P NMR chemical shifts using the SOS–DFPT–IGLO<sup>12</sup> and DFT–GIAO<sup>13</sup> methods. The electronic structures of the molecules were analyzed with the help of the NBO method.<sup>14</sup>

## Methods

The geometry optimizations have been carried out at the HF, MP2,<sup>15</sup> and DFT levels using the three-parameter fit of the exchange–correlation potential suggested by Becke (B3LYP).<sup>16</sup> The geometries of **7** and **8** could not be optimized at MP2 due to limited computational resources. Our standard basis set II, which has relativistic effective core potentials (ECP)<sup>17</sup> with (441/2111/N1) valence basis sets for Mo (*N* = 3) and W (*N* = 2) and 6-31G(d) all-electron basis sets for the first- and second-row atoms,<sup>18</sup> was employed for calculating geometries and bond energies.<sup>10</sup> ECPs with (31/31/1) valence basis sets have been used for phosphorus and sulfur.<sup>19</sup> The exponents for the d-type polarization functions are ζ(P) = 0.55 and ζ(S) = 0.65.<sup>20</sup> Single-point energy calculations of B3LYP/II-optimized structures have been performed using coupled-cluster theory<sup>21</sup> with singles and doubles and noniterative estimation of triple excitations, CCSD(T).<sup>22</sup> The geometry optimizations and frequency calculations at the HF level of theory were carried out with the help of Turbomole,<sup>23</sup> while the DFT and MP2 calculations were performed with Gaussian94.<sup>24</sup> For the CCSD(T) calculations the

program Molpro was employed.<sup>25</sup> The nature of the stationary points was investigated by calculating the Hessian matrices at the MP2/II level. Vibrational frequencies have not been calculated for **7** or **8** because of limited computational resources. All other structures reported here are minima on the potential energy surfaces (number of imaginary frequencies = 0).

Larger basis sets and a different DFT functional have been used for the calculations of the NMR chemical shifts and coupling constants. The Stuttgart ECPs with a standard 6s5p3d valence basis set for Mo and W<sup>26</sup> in conjunction with basis set III for the other atoms as proposed by Kutzelnigg<sup>27</sup> have been employed for the calculations of the shielding constants using the SOS–DFPT–IGLO method developed by Malkin et al.<sup>12</sup> Uncoupled DFT–GIAO calculations<sup>13</sup> using the Dunning–Huzinaga D95 full double-zeta basis set extended with two sets of polarization functions<sup>28</sup> and the Stuttgart ECPs for Mo and W have also been carried out. The BPW91 exchange–correlation potentials<sup>29</sup> were used for the chemical shift calculations as proposed by Malkin.<sup>30</sup> The program DeMon was used for the SOS–DFPT–IGLO calculations,<sup>31</sup> while Gaussian94<sup>24</sup> was employed for the uncoupled DFT–GIAO calculations. No corrections were introduced concerning the use of ECPs in the NMR chemical shift calculations.

## Geometries and Bond Energies

Figure 1 shows the optimized geometries of the model compounds **1**–**10** and the experimental values of the substituted derivatives **1a** and **8a**. A table with the calculated total energies and zero-point vibrational energies of the molecules is given as Supporting Information. Table 1 gives the calculated metal–S and metal–NH<sub>3</sub> bond dissociation energies.

A comparison of the theoretical geometries of **1** and **8** with the experimental data for **1a** and **8a** shows that the B3LYP/II-predicted metal–P bond lengths are in excellent agreement with experiment, while the HF/II values are too short and the MP2/II value for **1** is too long. It is generally known that multiple bonds are calculated too short at HF and too long at MP2.<sup>32</sup> It seems that B3LYP/II is the best choice to calculate interatomic distances of multiple bonds. The remaining bond lengths and N<sub>eq</sub>–M–P bond angles of **1** and **8** predicted at all levels of theory are in good agreement with the experimental results except for the W–N<sub>ax</sub> bond length of **8**. The experimental value for **8a** (2.34 Å) is significantly shorter than HF/II value (2.475

(10) Frenking, G.; Antes, I.; Böhme, M.; Dapprich, S.; Ehlers, A. W.; Jonas, V.; Neuhaus, A.; Otto, M.; Stegmann, R.; Veldkamp, A.; Vydroshchikov, S. F. In *Reviews in Computational Chemistry*; Lipkowitz, K. B., Boyd, D. B., Eds.; VCH: New York, Vol. 8, p 63.

(11) Berces, A.; Ziegler, T. *Topics in Current Chemistry*; Nalewajski, R. F., Ed.; Springer-Verlag: Berlin, 1996; Vol. 182, p 41f.

(12) (a) Malkin, V. A.; Malkina, O. L.; Salahub, D. R. *Chem. Phys. Lett.* **1993**, *204*, 87. (b) Malkin, V. A.; Malkina, O. L.; Casida, M. E.; Salahub, D. R. *J. Am. Chem. Soc.* **1994**, *116*, 5898.

(13) Schreckenbach, G.; Ziegler, T. *J. Phys. Chem.* **1995**, *99*, 606.

(14) Reed, A. E.; Curtiss, L. A.; Weinhold, F. *Chem. Rev.* **1988**, *88*, 899.

(15) (a) Møller, C.; Plesset, M. S. *Phys. Rev.* **1934**, *46*, 618. (b) Binkley, J. S.; Pople, J. A. *Int. J. Quantum Chem.* **1975**, *9*, 229.

(16) Becke, A. D. *J. Chem. Phys.* **1993**, *98*, 5648.

(17) Hay, P. J.; Wadt, W. R. *J. Chem. Phys.* **1985**, *82*, 299.

(18) (a) Hehre, W. J.; Ditchfield, R.; Pople, J. A. *J. Chem. Phys.* **1972**, *56*, 2257. (b) Hariharan, P. C.; Pople, J. A. *Theoret. Chim. Acta* **1973**, *28*, 213. (c) Gordon, M. S. *Chem. Phys. Lett.* **1980**, *76*, 163.

(19) Bergner, A.; Dolg, M.; Küchle, W.; Stoll, H.; Preuss, H. *Mol. Phys.* **1993**, *80*, 1431.

(20) Andzelm, J.; Huzinaga, S.; Klobukowski, M.; Radzio, E.; Sakai, Y.; Tatekawi, H. *Gaussian Basis Sets for Molecular Calculations*; Elsevier: Amsterdam, 1984.

(21) (a) Cizek, J. *J. Chem. Phys.* **1966**, *45*, 4256. (b) Cizek, J. *Adv. Chem. Phys.* **1966**, *14*, 35.

(22) (a) Pople, J. A.; Krishnan, R.; Schlegel, H. B.; Binkley, J. S. *Int. J. Quantum Chem.* **1978**, *14*, 545. (b) Bartlett, R. J.; Purvis, G. D. *Int. J. Quantum Chem.* **1978**, *14*, 561. (c) Purvis, G. D.; Bartlett, R. J. *J. Chem. Phys.* **1982**, *76*, 1910. (d) Purvis, G. D.; Bartlett, R. J. *J. Chem. Phys.* **1987**, *86*, 7041.

(23) (a) Häser, M.; Ahlrichs, R. *J. Comput. Chem.* **1989**, *10*, 104. (b) Ahlrichs, R.; Bär, M.; Häser, M.; Horn, H.; Kölmel, C. *Chem. Phys. Lett.* **1989**, *162*, 165. (c) Horn, H.; Weiss, H.; Häser, M.; Ehrig, M.; Ahlrichs, R. *J. Comput. Chem.* **1991**, *12*, 1058. (d) Häser, M.; Ahlrichs, R.; Feysereisen, M. W. *Theor. Chim. Acta.* **1991**, *79*, 115.

(24) Frisch, M. J.; Trucks, G. W.; Schlegel, H. B.; Gill, P. M. W.; Johnson, B. G.; Robb, M. A.; Cheeseman, J. R.; Keith, T. A.; Petersson, G. A.; Montgomery, J. A.; Raghavachari, K.; Al-Laham, M. A.; Zakrzewski, V. G.; Ortiz, J. V.; Foresman, J. B.; Cioslowski, J.; Stefanov, B. B.; Nanayakkara, A.; Challacombe, M.; Peng, C. Y.; Ayala, P. Y.; Chen, W.; Wong, M. W.; Andres, J. L.; Replogle, E. S.; Gomberts, R.; Martin, R. L.; Fox, D. J.; Binkley, J. S.; Defrees, D. J.; Baker, I.; Stewart, J. J. P.; Head-Gordon, M.; Gonzalez, C.; Pople, J. A. *Gaussian94*; Gaussian Inc.: Pittsburgh, PA, 1995.

(25) Werner, H.-J.; Knowles, P. J. Universität Stuttgart and University of Birmingham.

(26) Andrae, D.; Häusermann, U.; Dolg, M.; Stoll, H.; Preuss, H. *Theor. Chim. Acta* **1990**, *77*, 123.

(27) Kutzelnigg, W.; Fleischer, U.; Schindler, M. *NMR* **1990**, *23*, 167.

(28) Dunning, T. H.; Hay, P. J. *Modern Theoretical Chemistry*; Schaefer, H. F., III Ed.; Plenum: New York, 1976.

(29) (a) Becke, A. D. *Phys. Rev. A*, **1988**, *38*, 3098. (b) Perdew, J. P.; Wang, Y. *Phys. Rev. B* **1992**, *45*, 13244.

(30) Malkin, V. A.; Malina, O. L.; Salahub, D. R. *Chem. Phys. Lett.* **1993**, *204*, 87.

(31) (a) St.-Amand, A.; Salahub, D. R. *Chem. Phys. Lett.* **1990**, *169*, 387. (b) Salahub, D. R.; Fournier, R.; Mlynarski, P.; Papai, I.; St.-Amand, A.; Ushio, J. In *Density Functional Methods in Chemistry*; Labanowski, J., Andzelm, J., Eds.; Springer: New York, 1991; p 71.

(32) Hehre, W. J.; Radom, L.; Schleyer, P. v. R.; Pople, J. A. *Ab Initio Molecular Orbital Theory*; Wiley: New York, 1986.

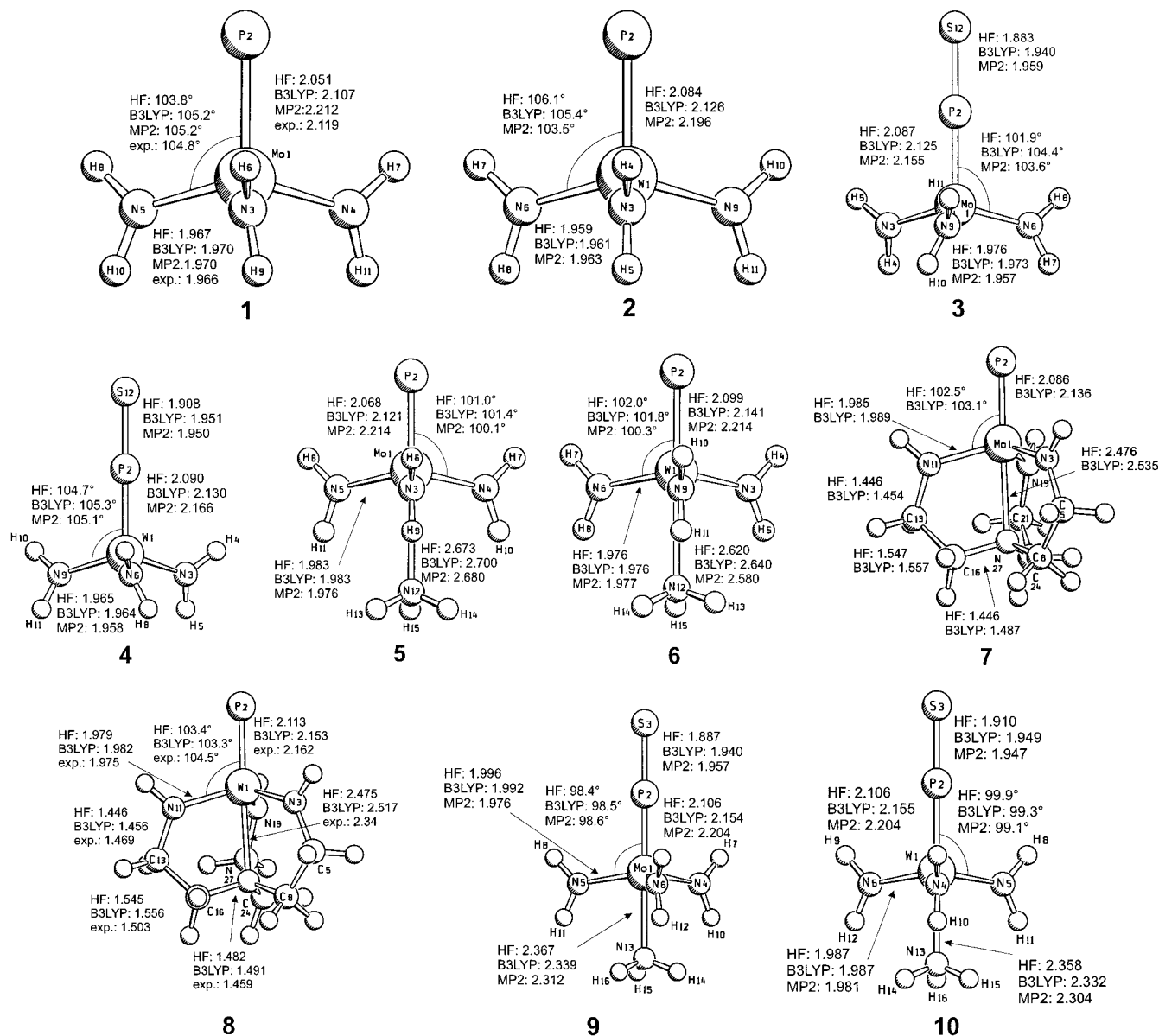


**Figure 1.** Theoretical and experimental geometries (distances in Å, angles in degrees). The experimental data for **1** and **8** are taken from the substituted analogues **1a** and **8a**, respectively (see refs 3 and 4).

**Table 1.** Theoretically Predicted Bond Dissociation Energies  $D_e$  and  $D_0$  (kcal mol<sup>-1</sup>) of the P–S and M–NH<sub>3</sub> Bonds

compound	$D_e(S)^{a,b}$				$D_e(NH_3)^c$				
	HF	MP2	B3LYP	CCSD(T) <sup>c</sup>	HF	MP2	B3LYP	CCSD(T) <sup>c</sup>	
[Mo(PS)(NH <sub>2</sub> ) <sub>3</sub> ]	<b>3</b>	28.2 (31.0)	34.6 (35.4)	57.9 (59.7)	47.6 (49.4)	—	—	—	—
[W(PS)(NH <sub>2</sub> ) <sub>3</sub> ]	<b>4</b>	19.8 (18.1)	37.4 (35.7)	50.3 (48.6)	42.2 (40.5)	—	—	—	—
[Mo(P)(NH <sub>2</sub> ) <sub>3</sub> (NH <sub>3</sub> )]	<b>5</b>	—	—	—	—	8.6 (6.0)	10.3 (7.7)	7.2 (4.6)	15.8 (13.2)
[W(P)(NH <sub>2</sub> ) <sub>3</sub> (NH <sub>3</sub> )]	<b>6</b>	—	—	—	—	10.5 (7.6)	16.0 (13.1)	8.9 (6.0)	17.4 (14.4)
[Mo(PS)(NH <sub>2</sub> ) <sub>3</sub> (NH <sub>3</sub> )]	<b>9</b>	41.2 (40.9)	53.9 (53.6)	71.6 (71.3)	62.9 (62.6)	21.6 (16.9)	29.6 (24.9)	22.8 (18.1)	31.2 (26.5)
[W(PS)(NH <sub>2</sub> ) <sub>3</sub> (NH <sub>3</sub> )]	<b>10</b>	33.2 (30.6)	56.0 (53.4)	66.4 (63.8)	58.5 (55.9)	24.0 (20.1)	32.4 (28.5)	24.9 (21.0)	33.7 (29.8)

<sup>a</sup> Values in parentheses give ZPE-corrected dissociation energies  $D_0$ . <sup>b</sup> Dissociation energies with respect to the <sup>3</sup>P ground state of S. <sup>c</sup> Using B3LYP/II optimized geometries.

Å) and the B3LYP/II value (2.517 Å). Part of the discrepancy between theory and experiment may be due to solid-state effects. The W–N<sub>ax</sub> bond has donor–acceptor character. It has been shown that the bond lengths of donor–acceptor complexes in

the solid state are *always* shorter than in the gas phase.<sup>33</sup> The shortening is mainly caused by dipole–dipole interactions in the solid state, and the weaker the donor–acceptor bond is the more it becomes shortened in the solid state.<sup>33</sup> Similar results

as presented here have been reported for the geometries of **1** and **8a**.<sup>5,8</sup> DFT calculations of **1** gave a Mo–P bond length of 2.108 Å, which is nearly the same as that calculated in our work.<sup>8</sup> A theoretical study of **8a** at the BP86 level of theory using relativistic ECPs and valence basis sets of DZP quality yielded a W–P bond length of 2.181 Å, which is in reasonable agreement with the experimental value.<sup>5</sup> The W–N<sub>ax</sub> distance, however, was 2.527 Å, which is also significantly longer than the experimental value.

The HF and B3LYP calculations predict that the sulfide complexes **3** and **4** have only slightly longer metal–P bonds and more acute N–M–P bond angles than **1** and **2**, while the M–N distances remain nearly the same. MP2 gives shorter M–P bonds for **3** and **4** than for **1** and **2**. We think that the B3LYP/II-predicted changes of the length of the multiple bonds are more reliable because of the known problems of MP2 for calculating bond lengths of multiple bonds.<sup>32</sup> Conflicting results at the MP2 and B3LYP levels of theory are also given for the P–S bonds of **3** and **4**. MP2/II gives a longer and weaker P–S bond for **3** than for **4**, while B3LYP predicts the opposite (Figure 1 and Table 1). Since B3LYP/II is more reliable than MP2/II for the bond lengths, we calculated the  $L_{M,MP}$ –S bond energies of **3** and **4** at CCSD(T)/II using the B3LYP/II-optimized geometries. The CCSD(T)/II/B3LYP/II values for the P–S bond energies are  $D_e = 47.6$  kcal/mol for **3** and  $D_e = 42.2$  kcal/mol for **4**. It follows that the CCSD(T)/II calculations support the relative P–S bond strengths of **3** and **4** as predicted at the B3LYP/II level, but the absolute values at DFT are too high.

Next, we calculated the NH<sub>3</sub> adducts of **1** and **2** leading to the complexes **5** and **6**. The theoretical results shown in Figure 1 and Table 1 suggest that the metal–NH<sub>3</sub> bonds are rather long and not very strong. The calculated bond energies at CCSD(T)/II/B3LYP/II are  $D_e = 15.8$  kcal/mol for **5** and  $D_e = 17.4$  kcal/mol for **6**. This is in reasonable agreement with the M–NH<sub>3</sub> bond energies calculated at MP2/II, while B3LYP/II gives values that are clearly too low (Table 1). At first sight it is surprising that B3LYP gives M–NH<sub>3</sub> bond dissociation energies that are too low, while the B3LYP values for the P–S bond energies are too high. This can be explained by the different type of bonds. The P–S bond is a covalent bond, while the M–NH<sub>3</sub> bond is a donor–acceptor bond. It is generally known that DFT frequently overestimates the bond strength of covalent bonds, while donor–acceptor bonds (particularly weak van der Waals bonds) are calculated too weak using DFT methods. MP2/II-calculated dissociation energies of donor–acceptor complexes are usually in good agreement with experiment.<sup>33</sup>

The metal–N<sub>ax</sub> donor–acceptor bonds of the related complexes **7** and **8** which have an N<sub>3</sub>N ligand are significantly shorter than the metal–NH<sub>3</sub> bonds of **5** and **6** (Figure 1). Part of the enhanced metal–N<sub>ax</sub> interactions may be due to the constrained cage structure of the N<sub>3</sub>N ligand, but part may be due to the nature of the amine nitrogen atom. The axial amine in **7** and **8** is a trialkyl amine, while the axial amine in **5** and **6** is ammonia. The donor–acceptor bonds of BF<sub>3</sub> and BCl<sub>3</sub> with NMe<sub>3</sub> are ~10 kcal/mol stronger than with NH<sub>3</sub>.<sup>33</sup> The stronger metal–N<sub>ax</sub> interactions in **7** and **8** lead to slightly longer metal–P bonds compared to **5** and **6** (Figure 1).

The calculated results for **9** and **10** are very interesting. The theoretically predicted geometries and bond energies show that the P–S bonds are significantly stronger than in **3** and **4** and

that the metal–N<sub>ax</sub> donor–acceptor bonds are also stronger than in **5** and **6**. The M–P bonds of **9** and **10** are longer compared to the respective bonds of **3–6**. It follows that the H<sub>3</sub>N–MPS and H<sub>3</sub>NMP–S bonds strengthen each other. This can be explained by the different bonding situations of the M–P bonds in the complexes. The metal–PS bonds in **3** and **4** are essentially double bonds, while the metal–P bonds in **1** and **2** are triple bonds (see below). This reduces the number of formal coordination sites being occupied at the metal in **3** and **4** to five, leaving one coordination site empty. The empty coordination site is filled in **9** and **10** with the amine ligand, leading to strong metal–amine bonding. There is no empty coordination site at the metal in **1** or **2**, which leads to much weaker metal–ammonia bonding in **5** and **6**. The amine ligand in return changes the polarity of the metal–P bond in **5** and **6** in such a way that the terminal phosphido ligand becomes more basic (see below), yielding stronger P–S bonding in **9** and **10** compared to **3** and **4**.

The theoretical P–S and M–NH<sub>3</sub> bond strengths of **9** and **10** given at the different levels of theory show the same trend as for **3–6**. The P–S dissociation energies at B3LYP/II have the right order, **9** > **10**, but the absolute values are 8–10 kcal/mol too high. The M–NH<sub>3</sub> bond energies at MP2/II are in good agreement with the CCSD(T)/II results, while the B3LYP/II values are clearly too low.

From the calculated bond strengths it follows that **7** and **8** should more easily react with sulfur than **1** and **2**, yielding the corresponding sulfide complexes. This theoretical prediction should be tested experimentally.

### <sup>31</sup>P NMR Chemical Shifts

The most important analytical method to identify new compounds is NMR spectroscopy. However, it is sometimes difficult to deduce the structure of a molecule solely from the observed NMR spectra without knowing the proper reference compounds. Theoretical methods would become even more important for experimental studies if the calculated NMR chemical shifts (and coupling constants) were accurate enough to examine the structural predictions which come up from the observed NMR spectra. There has been impressive progress in the development of reliable methods to compute NMR spectra in the last couple of years.<sup>12,13,34</sup> However, the accuracy of theoretically predicted NMR chemical shifts for such unusual and exotic compounds as **1–10** is not known, and it cannot be taken as granted that the calculated NMR values are reliable. Because the <sup>31</sup>P chemical shifts and even the chemical shift anisotropies (CSA) of some analogues have been measured, we calculated the theoretical values of **1–10** using the SOS–DFPT–IGLO and DFT–GIAO methods. Details are given in the Methods section.

Table 2 shows the calculated <sup>31</sup>P chemical shifts of **1–10** and experimental values for the substituted derivatives **1a**, **3a**, **7a**, and **8a**. The absolute values of the theoretically predicted and experimentally observed chemical shifts may be different not only because of limited accuracy of the theoretical method but also because the experimental values refer to substituted compounds and not to the parent molecules which have been calculated. Furthermore, the experimental values are subject to solvent effects. However, the trends in the theoretical and experimental data should be correct. Table 2 shows that this is

(33) Jonas, V.; Frenking, G.; Reetz, M. T. *J. Am. Chem. Soc.* **1994**, *116*, 8741.

(34) (a) Gauss, J. *Chem. Phys. Lett.* **1994**, *229*, 198. (b) Sugimoto, M.; Nakasuji, H. *J. Chem. Phys.* **1995**, *102*, 285. (c) Cremer, D.; Olsson, L.; Reichel, F.; Kraka, E. *Isr. J. Chem.* **1993**, *33*, 369 and references therein.

**Table 2.** Theoretical and Experimental Isotropic  $^{31}\text{P}$  Chemical Shifts ( $\delta$ )

compound		IGLO	GIAO	expt
[Mo(P)(NH <sub>2</sub> ) <sub>3</sub> ]	<b>1</b>	1057.4	1090.0	1216 <sup>a</sup>
[W(P)(NH <sub>2</sub> ) <sub>3</sub> ]	<b>2</b>	860.0	872.5	—
[Mo(PS)(NH <sub>2</sub> ) <sub>3</sub> ]	<b>3</b>	415.7	385.0	383 <sup>a</sup>
[W(PS)(NH <sub>2</sub> ) <sub>3</sub> ]	<b>4</b>	355.6	326.2	—
[Mo(P)(NH <sub>2</sub> ) <sub>3</sub> (NH <sub>3</sub> )]	<b>5</b>	1214.1	1214.5	—
[W(P)(NH <sub>2</sub> ) <sub>3</sub> (NH <sub>3</sub> )]	<b>6</b>	1004.2	1097.4	—
[Mo(P)(N <sub>3</sub> N)]	<b>7</b>	nc <sup>b</sup>	1183.5	1346 <sup>c</sup>
[W(P)(N <sub>3</sub> N)]	<b>8</b>	nc	951.3	1080 <sup>c</sup>
[Mo(PS)(NH <sub>2</sub> ) <sub>3</sub> (NH <sub>3</sub> )]	<b>9</b>	nc	318.9	—
[W(PS)(NH <sub>2</sub> ) <sub>3</sub> NH <sub>3</sub> ]	<b>10</b>	nc	270.3	—

<sup>a</sup> Values for **1a** and **3a**, respectively (ref 3). <sup>b</sup> nc, no convergence. <sup>c</sup> Values for **7a** and **8a**, respectively (ref 4).

the case. The experimental  $^{31}\text{P}$  value for **1a** (1216 ppm) is ~160–120 ppm higher than the IGLO and GIAO values for **1** (1057 and 1090 ppm, respectively). Theory and experiment agree that the  $^{31}\text{P}$  signal for **3** and **3a** is much lower. The nearly quantitative agreement between the experimental value (383 ppm) and the GIAO result (385 ppm) is fortuitous, however. The better agreement between the theoretical  $^{31}\text{P}$  value for **3** and the experimental result for **3a** compared to the values for **1** and **1a** can be explained with the much higher paramagnetic contribution to the chemical shift of the phosphido complexes. Larger basis sets than used in our work appear to be necessary for accurate determination of paramagnetic contributions. A previous study of **1** using the GIAO method with a large all-electron basis set for Mo and 6-311G(d,p) for the other atoms gave an isotropic  $^{31}\text{P}$  chemical shift of 1463 ppm, which is in better agreement with the experimental value than our result.<sup>8</sup>

The experimentally observed  $^{31}\text{P}$  chemical shift of **7a** is 130 ppm higher than in **1a**, while the  $^{31}\text{P}$  signal of **8a** is 136 ppm lower than in **1a** (Table 2). This is in good agreement with the calculated differences at the GIAO level. The  $^{31}\text{P}$  signal of **1** is 93 ppm lower than in **7**, and it is 139 ppm higher than in **8**. Unfortunately, the IGLO calculations of **7–10** did not converge. However, the trends predicted by the IGLO and GIAO methods for the compounds **1–6** are very similar. The phosphorus atoms carrying a terminal sulfide (**3**, **4**, **9**, **10**) are significantly more shielded than the respective terminal phosphorus atoms in **1**, **2**, **5**, and **6**. The  $^{31}\text{P}$  signals of the latter compounds are shifted 500–900 ppm to lower field (Table 2).

The good agreement between theory and experiment is also found for the anisotropies of the  $^{31}\text{P}$  values of **1**, **7**, **8**, and **1a**, **7a**, and **8a**, respectively. Table 3 shows that the component of the  $^{31}\text{P}$  chemical shift tensor which is parallel to the 3-fold axis of the compounds  $\delta_{\parallel}$  is much more shielded than the orthogonal component  $\delta_{\perp}$  of **1**, **7**, and **8**. This holds for the calculated and the experimental values of the substituted analogues. The

absolute values of the calculated CSA of **1** are lower (1857 ppm at the IGLO level, 1852 ppm at the GIAO level) than the experimental results for the substituted derivative **1a** (2311 ppm). A better agreement with experiment was obtained in a previous theoretical study of **1**, in which a larger basis set was used for the GIAO calculations.<sup>8</sup> The values for the parallel and orthogonal components of the  $^{31}\text{P}$  chemical shift tensor were 2228 and –67 ppm, respectively, which give a predicted CSA of 2295 ppm. Our calculated trends at the GIAO level for the components of the shift tensor and the CSA values for **1**, **7**, and **8** are in agreement with the experimental values for the respective analogues (Table 3). The calculations show that the terminal sulfide atom has a large effect on the perpendicular component  $\delta_{\perp}$  of the  $^{31}\text{P}$  chemical shift, while the parallel component  $\delta_{\parallel}$  is much less influenced (compare **1**, **2**, **5**, and **6** with **3**, **4**, **9**, and **10**). This is in agreement with experimental values for the  $^{31}\text{P}$  chemical shift tensors of several compounds containing a triply bonded phosphorus atom.<sup>8</sup>

### Analysis of the Chemical Bonding

Table 4 shows the calculated atomic partial charges of the molecules and the Wiberg bond orders<sup>35</sup> of the relevant bonds taken from the NBO partitioning scheme. The polarization and the hybridization of the metal–ligand and P–S bonds are given in Table 5.

The metal atoms of **1–10** carry always a significant positive partial charge, while the nitrogen atoms are clearly negatively charged. The terminal phosphorus atom of the phosphido complexes **1**, **2**, and **5–8** is nearly neutral, but the P atom of the phosphorus–sulfide complexes **3**, **4**, **9**, and **10** is positively charged because of P → S charge donation (Table 4). The sulfur atom of the sulfide complexes is negatively charged. The Wiberg bond indices show that the phosphido complexes have bond orders M–P = ~2.5, which become much lower in the phosphorus–sulfide complexes having bond orders M–P = 1.5–1.9. This is interesting because the optimized M–P bond lengths of the complexes with terminal phosphorus atoms are not very different from the M–PS interatomic distances (Figure 1). It should be noted that the Wiberg bond indices are a measure for the covalent bond order.<sup>35</sup> Considering the ionic contributions, the M–P bonds of the phosphido complexes are clearly triple bonds and the phosphorus–sulfide complexes have M–P and P–S double bonds.

Table 5 shows the NBO results for the most important bonds of **1–10**. We remind the reader that the NBO partitioning scheme searches for the most important Lewis structure of each compound. The results given in Table 5 indicate that the most important Lewis structure of **1–10** has a metal–phosphorus triple bond, i.e. even the phosphorus–sulfide complexes **3**, **4**,

**Table 3.** Experimental and Theoretical Anisotropies of the Calculated  $^{31}\text{P}$  Chemical Shifts

compound		IGLO			GIAO			expt		
		$\delta_{\parallel}$	$\delta_{\perp}$ <sup>a</sup>	$\delta_{\parallel} - \delta_{\perp}$	$\delta_{\parallel}$	$\delta_{\perp}$ <sup>a</sup>	$\delta_{\parallel} - \delta_{\perp}$	$\delta_{\parallel}$	$\delta_{\perp}$ <sup>a</sup>	$\delta_{\parallel} - \delta_{\perp}$
[Mo(P)(NH <sub>2</sub> ) <sub>3</sub> ]	<b>1</b>	–181.0	1676.6	–1857.6	–144.8	1707.6	–1852.4	–324	1987	–2311
[W(P)(NH <sub>2</sub> ) <sub>3</sub> ]	<b>2</b>	–211.7	1395.9	–1607.6	–187.9	1402.7	–1590.6	—	—	—
[Mo(PS)(NH <sub>2</sub> ) <sub>3</sub> ]	<b>3</b>	–292.6	769.8	1062.4	–268.4	711.7	–980.1	—	—	—
[W(PS)(NH <sub>2</sub> ) <sub>3</sub> ]	<b>4</b>	–267.3	667.1	–934.4	–247.8	613.1	–860.9	—	—	—
[Mo(P)(NH <sub>2</sub> ) <sub>3</sub> (NH <sub>3</sub> )]	<b>5</b>	–204.5	1755.9	–1960.4	–253.7	1948.5	–2202.2	—	—	—
[W(P)(NH <sub>2</sub> ) <sub>3</sub> (NH <sub>3</sub> )]	<b>6</b>	–295.9	1825.8	–2121.7	–240.1	1764.9	–2005.0	—	—	—
[Mo(P)(N <sub>3</sub> N)]	<b>7</b>	nc <sup>c</sup>	nc	nc	–96.0	1823.2	–1919.2	–267	2125	–2392
[W(P)(N <sub>3</sub> N)]	<b>8</b>	nc	nc	nc	–136.3	1495.0	–1631.3	–280	1728	–2008
[Mo(PS)(NH <sub>2</sub> ) <sub>3</sub> (NH <sub>3</sub> )]	<b>9</b>	nc	nc	nc	–402.0	679.4	–1081.4	—	—	—
[W(PS)(NH <sub>2</sub> ) <sub>3</sub> NH <sub>3</sub> ]	<b>10</b>	nc	nc	nc	–385.5	598.2	–983.7	—	—	—

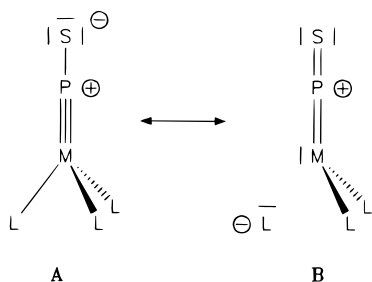
<sup>a</sup> Averaged over the two perpendicular components. <sup>b</sup> Experimental values for **1a**, **7a**, and **8a**, respectively (ref 8). <sup>c</sup> nc, no convergence.

**Table 4.** Calculated NBO Charges  $q$  and Wiberg Bond Indices  $B_{AB}$  of the B3LYP/II-Optimized Molecules

compound		$q$					$B_{AB}$			
		M	P	$N_{eq}$	$N_{ax}$	S	M-P	M- $N_{eq}$	M- $N_{ax}$	P-S
[Mo(P)(NH <sub>2</sub> ) <sub>3</sub> ]	<b>1</b>	0.70	0.13	-1.07	—	—	2.57	0.92	—	—
[W(P)(NH <sub>2</sub> ) <sub>3</sub> ]	<b>2</b>	1.00	-0.02	-1.12	—	—	2.62	0.91	—	—
[Mo(PS)(NH <sub>2</sub> ) <sub>3</sub> ]	<b>3</b>	0.73	0.52	-1.06	—	-0.40	1.84	0.93	—	1.61
[W(PS)(NH <sub>2</sub> ) <sub>3</sub> ]	<b>4</b>	1.16	0.26	-1.05	—	-0.33	1.50	1.12	—	1.45
[Mo(P)(NH <sub>2</sub> ) <sub>3</sub> (NH <sub>3</sub> )]	<b>5</b>	0.66	0.15	-1.16	-1.12	—	2.52	0.90	0.09	—
[W(P)(NH <sub>2</sub> ) <sub>3</sub> (NH <sub>3</sub> )]	<b>6</b>	0.94	0.00	-1.12	-1.12	—	2.56	0.90	0.11	—
[Mo(P)(N <sub>3</sub> N)]	<b>7</b>	0.63	0.12	-0.84	-0.55	—	2.46	0.86	0.11	—
[W(P)(N <sub>3</sub> N)]	<b>8</b>	0.90	-0.01	-0.90	-0.56	—	2.52	0.87	0.12	—
[Mo(PS)(NH <sub>2</sub> ) <sub>3</sub> (NH <sub>3</sub> )]	<b>9</b>	0.57	0.61	-1.06	-1.07	-0.42	1.76	0.89	0.24	1.66
[W(PS)(NH <sub>2</sub> ) <sub>3</sub> (NH <sub>3</sub> )]	<b>10</b>	0.86	0.51	-1.12	-1.09	-0.46	1.89	0.88	0.24	1.59

**Table 5.** Polarization and Hybridization of the Metal-Ligand and P-S Bonds at B3LYP/II Using the NBO Method

compound		bond M-L	% M	%s (M)	%p (M)	%d (M)	% L	%s (L)	%p (L)	%d (L)
[Mo(P)(NH <sub>2</sub> ) <sub>3</sub> ]	<b>1</b>	Mo-P ( $\sigma$ )	49.4	34.7	0.2	65.1	50.6	13.3	86.3	0.5
		Mo-P ( $\pi$ )	49.7	0.0	16.9	83.1	50.4	0.0	99.5	0.5
		Mo-P ( $\pi$ )	45.6	0.0	24.4	75.6	54.4	0.0	99.5	0.5
		Mo- $N_{eq}$	17.1	21.8	13.6	64.7	82.9	40.0	60.0	0.0
[W(P)(NH <sub>2</sub> ) <sub>3</sub> ]	<b>2</b>	W-P ( $\sigma$ )	47.5	35.0	0.2	64.9	52.5	14.9	84.6	0.5
		W-P ( $\pi$ )	46.7	0.0	16.2	83.8	53.3	0.0	99.5	0.5
		W-P ( $\pi$ )	43.2	0.0	22.8	77.2	56.8	0.0	99.5	0.5
		W- $N_{eq}$	15.9	21.7	12.9	65.5	84.1	41.8	58.1	0.0
[Mo(PS)(NH <sub>2</sub> ) <sub>3</sub> ]	<b>3</b>	Mo-P ( $\sigma$ )	25.8	46.9	0.3	52.8	74.2	59.5	40.5	0.0
		Mo-P ( $\pi$ )	61.4	0.0	0.3	99.7	38.6	0.0	99.4	0.6
		Mo-P ( $\pi$ )	61.5	0.0	0.3	99.7	38.5	0.0	99.4	0.6
		Mo- $N_{eq}$	23.7	17.3	0.5	82.2	76.3	25.4	74.6	0.0
		P-S	48.2	40.6	58.7	0.7	51.8	16.0	83.2	0.8
[W(PS)(NH <sub>2</sub> ) <sub>3</sub> ]	<b>4</b>	W-P ( $\sigma$ )	28.0	44.8	0.2	55.0	72.1	58.1	41.9	0.0
		W-P ( $\pi$ )	56.6	0.0	0.5	99.5	43.4	0.0	99.5	0.6
		W-P ( $\pi$ )	56.6	0.0	0.5	99.5	43.4	0.0	99.5	0.6
		W- $N_{eq}$	21.3	18.2	0.4	81.4	78.7	29.2	70.8	0.0
		P-S	49.6	41.6	57.7	0.7	50.4	15.1	84.1	0.8
[Mo(P)(NH <sub>2</sub> ) <sub>3</sub> (NH <sub>3</sub> )]	<b>5</b>	Mo-P ( $\sigma$ )	44.2	41.2	0.3	58.5	55.8	18.2	81.5	0.4
		Mo-P ( $\pi$ )	53.7	0.0	13.4	86.6	46.3	0.0	99.5	0.5
		Mo-P ( $\pi$ )	50.6	0.0	19.6	80.4	49.4	0.0	99.5	0.5
		Mo- $N_{eq}$	16.4	19.6	14.9	65.5	83.6	41.3	58.7	0.0

**Scheme 2.** Relevant Lewis Structures for  $L_n$ MPS Complexes<sup>a</sup>

<sup>a</sup> **A** is the most important Lewis form, although the bond indices suggest that the phosphido-sulfide complexes have  $L_nM=P=S$  double bonds.

**9**, and **10** should be written with a metal $\equiv$ PS triple bond and MP-S single bond. The apparent contradiction between the Wiberg bond indices, which suggest  $M=P=S$  double bonds, and the NBO picture with  $M\equiv P-S$  bonding is a representation problem. It is caused by the difficulty to write a reasonable Lewis structure for **3**, **4**, **9**, and **10** which has a  $M=P=S$  entity. Scheme 2 shows the most important Lewis structure **A** of the phosphorus-sulfide complexes as given by the NBO scheme. Lewis form **B** has a  $M=P=S$  moiety, but the necessity to formulate a lone-pair orbital at the metal makes this form less realistic than **A**. We emphasize that the bonding situation in  $L_n$ MPS complexes can also be considered as a  $L_nM\equiv PS$  triple

bond, which is more polarized and therefore weaker than in  $L_nM\equiv P$ , and a  $L_nMP-S$  single bond, which is additionally strengthened by ionic contributions. The sum of the three covalent contributions to the metal-PS bond then gives essentially a double bond. This leaves one formal coordination site at the metal empty in **3** and **4** but filled with a trans metal-NH<sub>3</sub> bond in **9** and **10**.

Examination of the NBO bond orbitals shows that the  $\sigma$  and  $\pi$  components of the metal-P triple bonds of the phosphido complexes **1**, **2**, and **5-8** are not very polarized to the metal or the phosphorus end (Table 5). The polarization changes significantly when a sulfur atom is bound to the phosphido ligand. The M-PS  $\sigma$  bonds of **3**, **4**, **9**, and **10** are clearly polarized toward the phosphorus end, while the M-PS  $\pi$  bonds become somewhat more polarized toward the metal. The P-S bonds are slightly polarized, while the metal- $N_{eq}$  bonds of all complexes are strongly polarized toward the nitrogen end. The metal-ligand  $\sigma$  bonds are mainly sd-hybridized at the metal, with small contributions from the metal p-AOs to some metal- $N_{eq}$  bonds.

Particularly interesting is the hybridization of the metal-phosphorus bonds. The low coupling constant for **8a**,  $J(P,W) = 138$  Hz, has been interpreted as an indication for a low  $\sigma$  contribution to the  $W\equiv P$ .<sup>4,7</sup> Table 5 shows that the s contribution at the phosphorus end of the M-P  $\sigma$  bonds of **1**, **2**, and **5-8** is indeed rather low ( $\sim 20\%$  s character), but the percentage of s contribution at the metal end is significant (35-40%). This is at variance with recently published theoretical results for **8a** using the PESH0 method,<sup>9</sup> which suggest that the M-P  $\sigma$  bond

has largely d character at the metal end.<sup>5</sup> The NBO results for the lone-pair orbitals of the terminal phosphorus atoms show that it has mainly s character. We want to point out that the s contributions to the M–PS bond of the phosphido–sulfide complexes **3**, **4**, **9**, and **10** at the metal and particularly the phosphorus end are clearly higher than in the phosphido complexes. It follows that the  $J(\text{P,W})$  coupling constants of the  $\text{L}_n\text{PS}$  complexes should be higher than in phosphido complexes  $\text{L}_n\text{P}$ . This prediction should be tested experimentally. Please note that the M–P  $\sigma$  bonds of **5** and **6** are more polarized toward the phosphorus end and the  $\pi$  bonds are more polarized toward the metal compared to **1** and **2** (Table 5). This makes the phosphido ligand of **5** and **6** more basic than in **1** and **2**, yielding stronger MP–S bonds in **9** and **10** than in **3** and **4**.

### Summary and Conclusion

The geometry optimizations at HF, MP2, and B3LYP using basis set II for the complexes **1–10** are in reasonable agreement with experimental results. From the few measured geometries it seems that B3LYP gives the best agreement with experiment. The metal–phosphorus triple bond length at HF is too short, and at MP2 it is too long. The  $\text{L}_n\text{MP–S}$  bond dissociation energies of **3**, **4**, **9**, and **10** predicted at B3LYP/II are 8–10 kcal/mol too high, but the trend for the metals  $\text{Mo} > \text{W}$  is in agreement with the CCSD(T)/II values. The metal– $\text{NH}_3$  bonds of **5** and **6** are not very strong. The P–S and M– $\text{NH}_3$  bonds of **9** and **10** are both significantly stronger than in **3–6** because

one formal coordination site at the metal in the  $\text{L}_3\text{MPS}$  complexes is empty and because the trans amine ligand polarizes the metal–P bond such that the phosphido ligand becomes more basic. The attachment of an amine ligand trans to the MPS bond strengthens the P–S bond and vice versa. The theoretical  $^{31}\text{P}$  NMR chemical shifts and anisotropies are in very good agreement with experimental values. Analysis of the electronic structure shows that the M–P bonds of the phosphido structure should be considered as true triple bonds. The  $\sigma$  and  $\pi$  components of the M–P triple bond become clearly more polarized in the  $\text{L}_n\text{MPS}$  phosphido–sulfide complexes. The bond orders suggest that the phosphido–sulfide complexes have  $\text{M}=\text{P}=\text{S}$  double bonds.

**Acknowledgment.** We thank the Deutsche Forschungsgemeinschaft (SFB 260-D19 and Graduiertenkolleg Metallorganische Chemie) and the Fonds der Chemischen Industrie for financial support. Excellent service was provided by the computer centers HRZ Marburg, HLRZ Darmstadt, HLRS Stuttgart, and HLRZ Jülich.

**Supporting Information Available:** One table listing the calculated total energies,  $E_{\text{tot}}$ , and zero point vibrational energies, ZPE, of **1–10**, ( $^{31}\text{P}$ )S, and  $\text{NH}_3$  (1 page). Ordering information is given on any current masthead page.

IC971139M